Articles in PresS. J Neurophysiol (August 13, 2008). doi:10.1152/jn.90635.2008

Title: Differential activity-dependent, homeostatic plasticity of two neocortical inhibitory circuits

Running Head: Differential activity-dependent plasticity of inhibitory circuits

Authors: Aundrea F. Bartley[1], Z. Josh Huang[2], Kimberly M. Huber[1], Jay R. Gibson[1]

[1]University of Texas, Southwestern Medical Center, Department of Neuroscience
Dallas, TX 75390-9111, USA

[2]Cold Spring Harbor Laboratory, Cold Spring Harbor, NY 11724, USA

Corresponding Author:

Jay R. Gibson
University of Texas, Southwestern Medical Center
Department of Neuroscience, Box 9111
Dallas, TX 75390-9111
Phone: 214-648-5133
Fax: 214-648-1801
Email: Jay.Gibson@UTSouthwestern.edu

8 figures, 4 supplementary figures
31 pages
abstract=262, intro=582 words

Keywords: Homeostasis, Inhibition, Synapse, Neocortex, Plasticity, Electrophysiology

Acknowledgements: This research was supported by the National Institute of Health grant (NS045711) (K.M.H), and supported by FRAXA Research Foundations (J.R.G., K.M.H.).

Abstract

Chronic changes in neuronal activity homeostatically regulate excitatory circuitry. However, little is known about how activity regulates inhibitory circuits or specific inhibitory neuron types. Here, we examined the activity-dependent regulation of two neocortical inhibitory circuits – parvalbumin-positive (Parv+) and somatostatin-positive (Som+) – using paired recordings of synaptically coupled neurons. Action potentials were blocked for 5 days in slice culture, and unitary synaptic connections among inhibitory/excitatory neuron pairs were examined. Chronic activity blockade caused similar and distinct changes between the two inhibitory circuits. First, increases in intrinsic membrane excitability and excitatory synaptic drive in both inhibitory subtypes were consistent with the homeostatic regulation of firing rate of these neurons. On the other hand, inhibitory synapses originating from these two subtypes were differentially regulated by activity blockade. Parv+ unitary IPSC (uIPSC) strength was decreased while Som+ uIPSC strength was unchanged. Using short duration stimulus trains, short-term plasticity for both uEPSCs and uIPSCs was unchanged in Parv+ circuitry while distinctively altered in Som+ circuitry - uEPSCs became less facilitating and uIPSCs became more depressing. In the context of recurrent inhibition, these changes would result in a frequency-dependent shift in the relative influence of each circuit. The functional changes at both types of inhibitory connections appear to be mediated by increases in presynaptic release probability and decreases in synapse number. Interestingly, these opposing changes result in decreased Parv+ mediated uIPSCs, but balance out to maintain normal Som+ mediated uIPSCs. In summary, these results reveal that inhibitory circuitry is not uniformly regulated by activity levels and may provide insight into the mechanisms of both normal and pathological neocortical plasticity.

Introduction

Neocortical activity levels are chronically altered during sensory map plasticity (Horton and Hubel 1981), neuronal circuit maturation (Turrigiano and Nelson 2004), and pathological conditions, such as epilepsy or stroke. To understand how activity modifies neural circuit properties during these conditions, we must know the cellular alterations occurring in different cell types. More specifically, we must know the role played by inhibitory neurons since they greatly influence network properties by controlling action potential generation and synaptic integration.

Across various species, most adaptations in neuronal properties in response to chronic activity level changes (minutes to days) appear to be homeostatic (Davis and Goodman 1998; Marder and Prinz 2002; Turrigiano and Nelson 2000). Regulation of cortical excitatory neurons, via synaptic and intrinsic membrane alterations, is usually consistent with the homeostatic maintenance of activity levels at a particular set-point (Desai et al. 2002; Desai et al. 1999b; Hartman et al. 2006; Hendry and Jones 1988; Kilman et al. 2002; Lissin et al. 1998; Marty et al. 2000; Micheva and Beaulieu 1995; Murthy et al. 2001; Turrigiano et al. 1998; Turrigiano and Nelson 2000). For example, excitatory drive onto individual excitatory neurons is increased after chronic action potential blockade. This is homeostatic because action potential generation is facilitated in order to regain the set-point for average activity.

While the activity-dependent regulation of neocortical inhibitory synapses has been commonly studied (Chattopadhyaya et al. 2004; Hartman et al. 2006; Kilman et al. 2002; Maffei et al. 2006; Maffei et al. 2004; Marty et al. 1997; Patz et al. 2003; Welker et al. 1989), little is known about how homeostasis is maintained in inhibitory neurons themselves. Unlike excitatory neurons, excitatory drive onto inhibitory neurons has been reported to be unchanged after activity blockade (Turrigiano et al. 1998). Similar to excitatory neurons, inhibitory neurons increase their intrinsic excitability in response to activity blockade (Desai et al. 1999a; Gibson et al. 2006).

However, neocortical inhibitory neurons are divided into subtypes which likely subserve different functions (Gibson et al. 1999; Reyes et al. 1998; Somogyi et al. 1998), and previous electrophysiological studies examining the homeostatic regulation of inhibitory neurons and their synapses have usually not made this distinction (but see (Maffei et al. 2004)). Due to their different roles in circuit function, different inhibitory subtypes and their synapses may be regulated differently by chronic changes in activity. Therefore, important questions remain. To what degree do different inhibitory neuron subtypes display homeostatic regulation of firing rate? To what degree are different synapse types differentially regulated by activity? Are the cellular mechanisms used to maintain homeostasis in different cell and synapse types similar?

Here, we investigated activity-dependent regulation of synapses involving two inhibitory subtypes – parvalbumin-positive (Parv+) and somatostatin-positive (Som+) neurons (Gonchar and Burkhalter 1997). These two subtypes have distinctly different electrophysiological and anatomical properties that suggest different roles in neocortical function. To determine how activity levels regulate the local functional connectivity to and from Parv+ and Som+ neurons, we performed dual recordings of synaptically coupled neuron pairs in neocortical slice cultures during chronic action potential blockade. The slice culture preparation effectively preserves the three dimensional structure, the different cell types, and the synaptic development that exists in cortical circuits *in vivo* (Chattopadhyaya et al. 2004; De Simoni et al. 2003; Gahwiler et al. 1997; Gorba et al. 1999; Stoppini et al. 1991) while also allowing control over activity levels. This experimental design provides insight into the regulation of local "recurrent" inhibition – the disynaptic pathway that includes the excitatory connection to the inhibitory neuron and the inhibitory connection back to the excitatory neuron.

Methods

Animals and Cell Identification Inhibitory neurons were identified by GFP fluorescence. In one line, GFP was only expressed in a subset of neocortical parvalbumin-positive (Parv+) inhibitory neurons (G42) (Chattopadhyaya et al. 2004). In another line, GFP was expressed only in a subset of somatostatin-positive (Som+) neurons (GIN mice, Jackson Laboratories) (Gibson et al. 2006; Oliva et al. 2000). The use of these mice for studying these biochemically defined neocortical inhibitory subtypes has been previously established (Chattopadhyaya et al. 2004; Di Cristo et al. 2004; Gibson et al. 2006; Oliva et al. 2000). We have previously confirmed the somatostatin expression of GFP neurons in GIN mice in our neocortical slice culture preparation (Gibson et al. 2006). In this study, no GFP-positive neurons ever elicited a uEPSC. In all dual recordings, the two GFP identified inhibitory subtypes displayed properties of action potential generation and afferent uEPSCs consistent with previous studies of the two subtypes (Gibson et al. 2006; Gibson et al. 1999; Reyes et al. 1998).

We acknowledge that these two categories may include different morphological subtypes (Dumitriu et al. 2007; Gupta et al. 2000). But when considering the consistent firing and synaptic properties that differentiate these two biochemical subtypes and the abundant anatomical and electrophysiological studies using these categories (Chattopadhyaya et al. 2004; Gibson et al. 2006; Gibson et al. 1999; Gonchar and Burkhalter 1997; Oliva et al. 2002; Reyes et al. 1998), this is a useful categorization.

Slice culture and Pharmacological Treatments: Preparation of interface slice cultures was based on a previous study (Stoppini et al. 1991). Mice (postnatal day 5-7; P5-7) were anesthetized with Halothane in a manner consistent with the recommendations of the Panel on Euthanasia of the American Veterinary Medical Association. The brain was removed and then dissected in a HEPES-based buffer containing kynurenic acid (1 mM) to obtain a square sheet of somatosensory neocortex, 2-3 mm on each side which was subsequently sliced into 400 um slices with a McIlwain chopper. Slices were transferred to 4°C culture media and then plated onto semiporous membranes (Millicell, Millipore) in warmed culture media. Slices were placed and

maintained in an incubator at 5% CO_2/35°C. Culture media was exchanged the next day and every 2 days thereafter. The first 2 exchanges involved adding a mitotic inhibitor to the culture medium (FUDR, 35 μM; uridine, 80 μM). Culture media (based on (Musleh et al. 1997)) was 20% adult horse serum (Hyclone, defined, SH 30074.02) and 80% MEM (GIBCO, 51200-020) and contained the following (in mM): 1 Glutamine (Glutamax, Invitrogen), 0.7 Ascorbic Acid, 1 $CaCl_2$, 2 $MgSO_4$, 12.9 Dextrose, 5.3 $NaCO_3$, 30 HEPES, 1 μg/ml bovine insulin (Sigma), pH 7.3, 315 mOsm. Slice culture age was termed "equivalent day" (ED) which is the sum of "days in vitro" (DIV) and the postnatal age (P) of the dissected mouse.

Chronic activity-blockade was mediated by 5 day tetrodotoxin (TTX, 2 μM) treatment beginning at ED15-20. Slices were refreshed with TTX once per day. After 5 days of blockade, neurons appeared as healthy as controls. Images of live slice cultures under DIC microscopy did not appear any different. Electrophysiological properties were normal since neurons had stable, subthreshold resting potentials, fired action potentials, displayed spontaneous synaptic events, and displayed evoked synaptic transmission. This is consistent with another study using 6 day TTX treatment of cortical slice cultures which reported no change in pyramidal cell density using anatomical markers (Chattopadhyaya et al. 2004).

As in other studies and other culture preparations, we have previously shown that these neocortical slice cultures display spontaneous activity and that chronic TTX application increases this spontaneous activity (Echevarria and Albus 2000; Gibson et al. 2006; Turrigiano 1999). Frequency of spontaneous population events was similarly high in the present study when we made no effort to suppress it (~1 event/30 sec). This spontaneous activity might affect synaptic measurements so we added compounds to suppress activity (see *Evoked unitary responses* below).

Electrophysiology: Unitary postsynaptic currents (uEPSCs and uIPSCs) were measured using simultaneous (dual) whole-cell recordings in cultured slices at 21°C in a submersion recording chamber. Slice age was ED20-25 unless stated otherwise, and all recordings were in layer 2/3.

Neurons were within 20 μm of each other and typically 8-20 μm below the surface. Recordings were performed with IR-DIC visualization (Stuart et al. 1993) using a Nikon E600FN microscope and a CCD camera (Hamamatsu). Resting membrane potential and series resistance were continuously measured to monitor recording stability. Cell capacitance was always measured at recording onset (filtered at 30 kHz, sampled at 50 kHz). Capacitance and input resistance were measured in voltage clamp with a 400 ms, -10 mV step from a -60 mV holding potential. The capacitance was calculated by first obtaining the decay time constant of a current transient induced by the -10 mV step (the faster time constant of a double-exponential decay fitted to the first 60 ms) and then dividing this by the series resistance. Data were not corrected for junction potential.

Electrophysiology solutions: ACSF contained (mM): 126 NaCl, 3 KCl, 1.25 NaH_2PO_4, 2 $MgSO_4$, 26 $NaHCO_3$, 25 dextrose, and 2 $CaCl_2$. Drugs were added to the ACSF to suppress activity (see *Evoked unitary responses* below). ACSF is saturated with 95% O_2 / 5% CO_2. The following were the pipette solutions (mM): K-Gluc = 130 K-gluconate, 6 KCl, 3 NaCl, 10 HEPES, 0.2 EGTA, 4 ATP-Mg, 0.3 GTP-Tris, 14 phosphocreatine-Tris, 10 sucrose. Cs-Meth = 140 Cs-methanesulfonate, 10 HEPES, 2.5 BAPTA, 4 ATP-Mg, 0.3 GTP-Tris, 14 phosphocreatine-Tris, 10 sucrose, 2 QX-314-Cl, 2 TEA-Cl; K-Gluc (High Cl) = 80 K-gluconate, 32 KCl, 6 NaCl, 10 HEPES, 0.1 EGTA, 4 ATP-Mg, 0.3 GTP-Tris, 14 phosphocreatine-Tris, 15 sucrose. Junction potentials were 9, 10, and 7 mV, respectively. Data were not corrected for junction potential. All pipette solutions were adjusted to pH 7.25, 290 mOsm.

Evoked unitary responses: For all uPSCs, the presynaptic cell was recorded with K-Gluc pipette solution. The standard presynaptic action potential (AP) train protocol was a 5 pulse, 20 Hz train applied every 8 seconds. Presynaptic action potentials were evoked in voltage clamp by a +20-+40 mV step for 8 ms and could be evoked probably because of the inability to voltage clamp at the AP initiation sites.

For uEPSCs, Cs-Meth pipette solution was used in the postsynaptic inhibitory neuron to reduce effects of intrinsic membrane alterations induced by TTX treatment. As a result of prolonged TTX treatment the spontaneous activity of the slices was high, therefore the following were added to the ACSF to decrease spontaneous activity: NBQX (0.05 μM), zolpidem (0.1 μM), and AP5 (100 μM). The NBQX reduced excitatory responses by approximately 15-20% ((Kumar et al. 2002) and our observations). The effects of TTX on synaptic parameters were not dependent on these additions to the ASCF, because similar results were obtained if recordings were performed in a high divalent ACSF (Supp. Figs. 1,2).

Unless stated otherwise, Parv+ mediated uIPSCs were measured with "high Cl^-" KGluc pipette solution at a -65 mV holding potential to enhance responses. Som+ mediated uIPSCs were performed with normal K-Gluc pipette solution at a holding potential of -55 mV because the response polarity varied between recordings with the "High Cl^-" version perhaps due to variability in diffusion of pipette solution into distal dendrites where Som+ inhibitory synapses are located. DNQX (20 μM) and AP5 (100 μm) was added when measuring uIPSCs. A potential unitary connection was considered connected if the average response was greater than 2 pA.

Coefficient of variation (CV) analysis was performed only on uEPSCs whose average was greater than 5 pA. The CV was calculated as follows: $(StdDev_{Resp}-StdDev_{Noise})/(Avg\ Response)$ (Beierlein et al. 2003; Faber and Korn 1991). $StdDev_{Noise}$ was measured at baseline approximately 10-15 ms before uEPSC onset with the same fixed baseline-to-peak window employed for response measurements.

mEPSC and Sr^{2+} Experiments: Miniature EPSCs (mEPSCs) were measured with TTX , picrotoxin, and AP5 in the bath. Strontium experiments were performed by replacing 2/2 mM Ca^{2+}/Mg^{2+} with 4/4 mM Sr^{2+}/Mg^{2+} (Gil et al. 1999). Asynchronous events induced by action potential trains in Sr^{2+} were measured in a 400 ms window. For Parv+ mediated uIPSCs, the window started at 350 ms relative to train offset and events were clearly not contaminated by spontaneously occurring events. For uEPSCs targeting Som+ neurons, the window started at 40

ms, and we calculated that approximately 5 out of 6 events were actual evoked quanta. Trains in Sr^{2+} experiments were 50 Hz and typically between 15 and 20 APs in length for Parv+ uIPSCs and Som+ uEPSCs. Synaptic quantal events from both mEPSC and Sr^{2+} experiments were analyzed using "Mini Analysis Program" (Synaptosoft) using a 9.5 and 7 pA detection threshold, respectively.

Intrinsic membrane properties: Recordings examining the intrinsic membrane properties were performed with K-Gluc pipette solution.

Som+ Bouton Counts: In slice cultures made from GIN mice, single isolated excitatory neurons were transfected with DsRed using single cell electroporation (SCE) (Haas et al. 2001; Rae and Levis 2002; Rathenberg et al. 2003). Approximately 8 to 10 days after plating, slices were removed from the incubator for 30 minutes for electroporation. SCE was accomplished using a glass micropipette filled with plasmid-containing solution. Resistance of the micropipette was between 15-20 MΩ when filled with saline containing 149.2 mM NaCl, 4.7 mM KCl, 5 mM HEPES, and 2.5 mM $CaCl_2$. A silver wire was placed inside the micropipette in contact with the 25 ng/μL DNA solution (pDS-Red2, Clontech). The insert containing the neocortical slice was placed in a customized chamber filled with Tyrode Solution containing 150 mM NaCl, 3 mM KCl, 2 mM $MgSO_4$, 10 mM HEPES, 10 mM dextrose, and 2 mM $CaCl_2$. To prevent both the tip from clogging and the dilution of the DNA, positive-pressure was applied to the pipette. The micropipette tip was slowly advanced towards the visualized cell while pipette resistance was constantly monitored with an applied square wave. When resistance increased ~25%, the SCE pulse protocol was performed. The electroporation pulse parameter protocol was a single train of 200 square pulses of 1 ms duration at 200 Hz with an amplitude of -5V. Approximately 2 cells per slice expressed the plasmid. Robust expression occurred after 24 hours, and both imaging and electrophysiological data indicated these cells were healthy after 10-14 days post transfection. Imaging confirmed that the neurons were excitatory by high spine density. After

electroporation, slices were returned to the incubator. Two or three days later, TTX treatment was initiated.

After 5 days, GFP-positive axons/boutons and DsRed-positive somas/dendrites were imaged in live slices using 2-photon microscopy (40x, Axioskop 2 FS, Zeiss). Specimens were excited with 910 nm light (Chameleon standard laser, Coherent), and optical sections were approximately 0.8 μm thick, imaged with a 0.8 μm spacing, and collected within 30 μm of the slice surface. Two to three axons were chosen per image stack that were between 20 to 25 μm in length. Boutons along an axon were identified by using a 1.5x threshold brightness relative to the axon, and by requiring that this increase be maintained for at least 250 nm (Fig. 8C). "Putative" synaptic contacts were identified based on a previous study (Di Cristo et al. 2004). A DsRed dendrite was analyzed across a 25 μm length for any "putative" synapses. Each "putative" contact was determined by an overlap of at least 500 nm between the green and red signal in the plane for which the green signal was the highest (Fig. 8E). These criteria have been shown to accurately identify synapses approximately 82% of the time (Di Cristo et al. 2004). Laser power was set at a point where additional power did not reveal additional axons on spines. The experimenter was blind to the treatment history of the slices when images were collected and when analyzed.

Drugs: Fast synaptic transmission was blocked with the following: N-methyl-D-aspartate (NMDA) receptor antagonist AP5 (100 μM, Sigma), the AMPA/Kainate receptor antagonists DNQX (20 μM, Sigma) and NBQX (0.05 μM, Sigma), and the $GABA_A$ receptor antagonist picrotoxin (100 μM, Sigma). When examining uEPSCs, GABAergic transmission was enhanced with the GABA-receptor inverse agonist, zolpidem (0.1 μM, Sigma). Chronic activity blockade was performed with tetrodotoxin (TTX, 2 μM, Sigma).

Analysis: All comparisons required data collection from "sister" - slice cultures originating from one preparation (one animal). Statistical significance was $p<0.05$, and all error bars in figures are SEM. Unless otherwise stated, statistical comparisons were determined by the unpaired t-test (Mann-Whitney) and, for greater than 2 groups, a one-way ANOVA followed by Fisher's PLSD

(multicomparisons). A chi-square test was applied to determine changes in the percent of connected pairs, and a Fishers Exact P-value was used to determine significance. All statistics were performed with Statview software (SAS). Sample number (n) is either cell number or unitary connections tested and is always given in the following order: Control, TTX-treated. Numbers in graphs are sample number.

Results

To determine how activity regulates Parv+ and Som+ inhibitory circuitry, we examined neurons in slice cultures that had undergone 5 days of chronic action potential blockade by a pharmacological compound (TTX, 2 μM). Electrophysiological properties were measured using simultaneous whole-cell recordings of neighboring excitatory/inhibitory neuron pairs.

Chronic activity blockade increases intrinsic membrane excitability of excitatory and inhibitory neurons

Activity blockade caused an increase in input resistance in all 3 cell types examined (Parv+, Som+, Exc), with the greatest change occurring in excitatory and Som+ neurons (75% and 63% increase, $p<0.0001$,. Supp. Table I), and comparatively little change in Parv+ neurons (19%, $p<0.01$).

Previous studies have demonstrated that the intrinsic membrane excitability of both Som+ and excitatory neurons increases with activity blockade (Desai et al. 1999b; Gibson et al. 2006). Increases in input resistance in all cells studied here are consistent with this process, and we have previously demonstrated that an increase in input resistance increases the excitability in Som+ neurons in an almost identical experimental paradigm (Gibson et al. 2006). To see if the same is occurring for Parv+ and excitatory neurons, we examined one metric for excitability -

threshold current to evoke an action potential. Consistent with the increased excitability hypothesis, both Parv+ and excitatory neurons had decreased thresholds (52% and 50% decrease, $p<0.0002$, 279±33 vs. 134±18 pA and 82±6 vs. 41±3 pA. Supp. Table I). Therefore, all cell types examined in this study display increased intrinsic membrane excitability with chronic action potential blockade.

Excitatory neurons uniquely displayed a significant 26% decrease in capacitance (25.9±1.7 vs. 19.2±1.3 pA, $p<0.004$, n=71,58), suggesting either that total membrane surface area is smaller after activity blockade or the intrinsic membrane capacitance is decreased. Very little change occurred in resting membrane potential for all cell types (See Supp. Table I for all membrane properties).

Local, unitary excitatory synaptic input onto Som+ and Parv+ neurons is increased after chronic activity blockade

We next examined local excitatory input onto Parv+ and Som+ neurons. Trains of action potentials were evoked in a presynaptic excitatory cell (5 APs, 20 Hz) and the resulting unitary EPSCs (uEPSCs) examined. We examined the first uEPSC in the train (uEPSC1) which represents "low frequency" transmission at these synapses since the previous response occurred 8 seconds previously. As observed in acute slices, the uEPSCs targeting Parv+ and Som+ cells had different durations at half-height (4.5±0.9 vs. 13.8±3.7 ms, $p<0.03$; n=10,11; uEPSC1) (Beierlein et al. 2003).

Both inhibitory neuron types showed a similar upregulation in excitatory input (Fig. $1A_1$,B_1). First, the percent of all cell pairs that had a detectable unitary connection, or "percent connected", was increased for Parv+ uEPSCs (Fig. $1A_2$). In addition, TTX induced a trend towards increased connectivity of Som+ uEPSCs (Fig. $1B_2$), and a statistically significant

increase was confirmed in additional experiments (see Fig. 5). Next, we measured the amplitude of the first uEPSC in the train (uEPSC1) to assay connection strength when a connection existed. Amplitude was dramatically larger in both cell types (Fig. $1A_3$,B_3). We then derived an excitatory drive value which was the average uEPSC1 amplitude including "nonconnections" (0 pA). By combining the effects of increased connectivity and increased amplitude, excitatory drive increased dramatically by approximately 3-fold for both inhibitory subtypes (Fig. $1A_4$,B_4). For Som+ neurons, we were able to determine that these changes were likely due to an arrest of normal activity-dependent development. This is based on our findings that uEPSC properties measured in immature Som+ neurons resemble TTX treated mature neurons (Supp. Fig. 3). Because increased excitatory drive induced by chronic activity blockade has previously been reported in excitatory neurons (Turrigiano et al. 1998), our data suggest that this may be a universal adaptation among all cortical neuron types.

Inhibitory synaptic transmission from Som+ and Parv+ neurons are differentially regulated by chronic activity blockade

Next, we examined local inhibition in excitatory neurons provided by Parv+ and Som+ subtypes. Trains of action potentials were evoked in the presynaptic inhibitory neuron (8 APs, 20 Hz) and again, we first examined low frequency transmission by focusing on uIPSC1 in the train. Parv+-mediated IPSCs were large and inward since we used a high Cl^- K-Gluc pipette solution. But this was not possible for Som+ uIPSCs because with the same solution, the polarity of the uIPSCs was not consistent (see Methods). Therefore, we used a normal Cl^- K-Gluc internal that resulted in outward Som+ uIPSCs.

Activity blockade differentially affected inhibitory connection strength based on inhibitory subtype (Fig. $2A_1$,B_1). First, the "percent connected" of all cell pairs tested was decreased for Parv+ uIPSCs and unaffected for Som+ uIPSCs (Fig. $2A_2$,B_2). No change in

uIPSC1 amplitude was detected for either cell type (Fig. $2A_3$,B_3). The net result of these changes is a 30% decrease in local inhibitory drive provided by Parv+ neurons and no change for that provided by Som+ neurons (Fig. $2A_4$,B_4). The difference in pipette solution cannot account for the results since additional experiments using the identical pipette solution for both uIPSC types revealed the same differential regulation (Supp. Fig. 2). While the rise time and width at half height of uIPSC1 were unchanged at Parv+ connections, the width of Som+ uIPSC1 was increased 22% (15.2±0.7 vs. 18.6±1.0 ms, $p<0.02$, n=25,32), suggesting that the total charge may have been enhanced in these responses. This latter alteration may be indicative of a change in subunit composition or our inability to effectively voltage clamp distally located Som+ synapses, but this was not examined further.

Short-term plasticity of disynaptic, recurrent inhibition is differentially affected by chronic activity blockade conferring a frequency-dependent regulation

Because the short-term dynamics of synaptic connections determines their information processing capabilities (Abbott et al. 1997; Tsodyks and Markram 1997) and provides information about the pre- or postsynaptic locus of plasticity, we measured the short-term plasticity of both EPSCs and IPSCs with short stimulus trains (Fig. 3,4). Interestingly, while plasticity of synapses associated with Parv+ circuitry was unchanged with activity blockade (Fig. 3A,4A), that of Som+ circuitry changed dramatically. Excitatory responses targeting Som+ neurons became much less facilitating (Fig. $3B_{1,2}$) and IPSCs originating from Som+ neurons became more depressing (Fig. $4B_{1,2}$). The last PSC in the train can be considered to represent high frequency transmission since it followed the previous response by only 50 ms. Therefore, the changes in short-term plasticity suggest that the relative magnitude of low and high frequency transmission was altered in Som+ circuitry. Specifically, there is a frequency-dependent shift in the relative contribution of Parv+ and Som+ mediated recurrent inhibition after chronic activity

blockade where Som+ neurons contribute more at lower frequency network activity. The increase in short-term depression at Som+ uIPSCs appeared to be an induced change, and not a developmental arrest, as revealed by recordings before treatment (Supp. Fig. 3).

EPSC increases onto Som+ neurons are due to increased presynaptic release probability and synapse number

.

We examined possible underlying synaptic mechanisms mediating the changes in excitatory synaptic function just described. First, consistent with the smaller set of data illustrated earlier (Fig. 1), additional recordings showed that the percent connectivity of uEPSCs onto Parv+ and Som+ subtypes was increased after activity blockade (Fig. $5A_1$,B_1). If synaptic formation is a statistically independent process, this suggests that the increase in excitatory drive onto these cells is at least partially mediated by an increase in synapse number. However, investigation of action potential-independent miniature EPSCs (mEPSCs) revealed no change onto either Parv+ or Som+ neurons (Fig. $5A_2$,B_2). Either mEPSCs did not reflect changes in evoked transmission (Calakos et al. 2004; Reim et al. 2001; Sara et al. 2005) or any changes in the locally derived synapses mediating our measured uEPSCs are masked by compensating changes from other afferents.

We performed further analysis and experiments investigating the mechanisms of uEPSC changes, but we only focused on Som+ neurons since similar experiments in Parv+ neurons were more variable and inconclusive. First, to determine if increases in uEPSCs were consistent with increased quantal content (a property dependent on synapse number and release probability), we measured the coefficient of variation (CV) and failure rate of uEPSCs. In addition to increased synapse number after blockade, the decrease in uEPSC facilitation at Som+ neurons also suggested that release probability was increased. Therefore, quantal content should be higher, and we expected a lower CV and a decreased failure rate. This indeed was the case (Fig. 6A,B).

Finally, we measured the quantal amplitude of synapses comprising these uEPSCs by substituting Ca^{2+} with Sr^{2+}. Sr^{2+} induces asynchronous release of presynaptic vesicles enabling the measurement of individual quantal events and therefore the strength of individual synapses (Fig. 6C). Quantal amplitude was subtly decreased after blockade (Fig. 6D), and therefore cannot account for the increased uEPSC size. In conclusion, increases in excitatory drive onto Som+ neurons after chronic blockade are most likely due to an increase in quantal content which, is mediated by increased presynaptic release probability and/or synapse number.

Activity blockade induces opposing changes at Parv+ inhibitory synapses: increased release probability and decreased synapse number

We next examined possible underlying synaptic changes at Parv+ mediated inhibitory synapses. Additional experiments revealed a clear decrease in the percentage of connected pairs, which suggests a decrease in synapse number after chronic blockade (Fig. 7A). If the decrease is strictly mediated by synapse number, we would expect no change in the quantal amplitude. In support of this idea, measurements of quantal amplitude during Sr^{2+} induced asynchronous release revealed no change (Fig. 7B). Therefore, decreased Parv+ uIPSCs after chronic blockade are likely due to a decrease in synapse number which is consistent with a previous anatomical study demonstrating decreases in Parv+ inhibitory synapse number after 5 day activity blockade in an almost identical preparation of neocortical slice culture (Chattopadhyaya et al. 2004).

Because short term plasticity of Parv+ uIPSCs was unaffected by chronic activity blockade, this appears to rule out any changes in presynaptic release probability (Fig. 4A). However, previous studies find that alterations in release probability are only detected at Parv+ uIPSCs using longer trains of action potentials (Kraushaar and Jonas 2000; Luthi et al. 2001). Therefore, to better determine if Parv+ synapses undergo changes in release probability, we performed experiments using long trains (15 Hz, 750 pulses, Fig 7C). With chronic activity

blockade, Parv+ uIPSCs became more depressing during longer stimulus trains, implicating increases in release probability (Fig. 7C). Therefore, increased release probability at Parv+ synapses may partially offset the effects of downregulated synapse number.

If increased release probability after activity blockade is masking the full functional effect of decreased synaptic number, then artificially increasing release probability closer to a ceiling should reveal greater decreases in Parv+-mediated uIPSCs. To test this idea, we increased release probability to ~80% of maximum by using 6 mM Ca^{2+} in the recording ACSF (Kraushaar and Jonas 2000). While Parv+ mediated uIPSCs observed in normal (2 mM Ca^{2+}) displayed no difference in amplitude (Fig. $2A_3$), those recorded in 6 mM Ca^{2+} were decreased by about 2-fold after blockade (Fig. 7D). Therefore, these data support the assertion that increased release probability and decreased synaptic number both occur with activity blockade, but functionally their effects offset each other. These data illustrate the diverse, and sometimes functionally opposing changes that synapses undergo in response to chronic activity changes.

Activity blockade also induces opposing changes at Som+ inhibitory synapses: increased release probability and decreased synapse number

Functional measurements of Som+ inhibitory synapses also suggested the existence of opposing synaptic changes during activity blockade. The increase in short-term depression of Som + uIPSCs suggested that release probability may be increased. This would be expected to increase uIPSC1, but instead we observed no change (Fig. $2B_{3,4}$). Unlike Parv+ synapses, the percent of connected cell pairs was unchanged (Fig. 8A). However, there may still be decreases in the number of synapses per connection (see below). To examine this possibility, we counted the number of Som+ (identified as GFP+) axon puncta, or swellings, and their contact frequency with excitatory neuron dendrites in live slices (Fig. 8; See Methods). These were considered "putative" presynaptic boutons and "putative" synaptic contacts, based on a previous study that

validated this method in neocortical slice cultures from the same mouse line (Di Cristo et al. 2004) (Fig. 8B; see Methods). Furthermore, other studies have used similar approaches of identifying "putative" synaptic contacts through visualization of closely opposed processes (Feldmeyer et al. 1999; Feldmeyer et al. 2002; Markram et al. 1997). To visualize and identify single isolated excitatory neurons, we expressed DsRed using single cell electroporation. The number of "putative" synaptic contacts were quantified by counting the number of points that GFP+ puncta colocalized with DsRed+ dendrites (for criteria, see Methods and Fig. 8E). A previous study observed that this method correctly identifies Som+ synaptic contacts 82% of the time (Di Cristo et al. 2004). Activity blockade reduced both the number of putative presynaptic boutons and synaptic contacts (Fig. 8D,F). It is unlikely that these effects are due to decreases in GFP expression since soma GFP intensity was unaffected by TTX treatment (n=56,43). Therefore, chronic activity blockade reduces Som+ synapse number similar to Parv+ synapses.

However, unlike Parv+ inhibitory synapses the local connection frequency of Som+ synapses with neighboring neurons is maintained with chronic activity blockade. The reasons for this difference is unclear, but may be due to a high number of Som+ synapses mediating a single unitary connection such that decreases in synapse number do not result in a detectable decrease in connection frequency. The high synapse number mediating connectivity is supported by the fact that Parv+ and Som+ uIPSC1 size is the same when the same pipette solution is used (Supp. Fig. 2) even though Som+ uIPSCs would be expected to be smaller due to their preferred targeting of distal dendrites (Di Cristo et al. 2004; Somogyi et al. 1998).

In summary, these results suggest that Som+ uIPSC1 drive remains unchanged because of the offsetting affects of increased release probability and decreased synapse number. Because single quantal events evoked with Sr^{2+} substitution were unresolvable at this connection, changes in quantal amplitude or individual synaptic strength to the contribution of postsynaptic synapse strength to this regulation remains unknown. In summary, a reduction in synapse number and an increase in release probability are sufficient to explain the homeostatic alterations at both Parv+

and Som+ inhibitory synapses. However, a different functional outcome occurs in the two subtypes.

Discussion

Here, using paired recordings of synaptically coupled neurons in neocortical slice culture we have identified robust activity-dependent regulation of two inhibitory circuits. Chronic activity blockade induced increases in excitatory drive and intrinsic excitability in both Parv+ and Som+ inhibitory neurons demonstrating homeostatic plasticity occurs in all cell types, both excitatory and inhibitory. In contrast, there is differential regulation of uIPSCs from Parv+ and Som+ neurons in response to activity blockade. Net inhibitory drive originating from Parv+ neurons were decreased while that from Som+ neurons was unchanged. In addition, there was differential frequency-dependent regulation of Parv+ and Som+ circuitry. Short-term plasticity of both EPSCs and IPSCs associated with Som+ circuitry became less facilitating (or more depressing), whereas, short-term plasticity (of short trains) of Parv+ synapses was unaffected. Therefore, at low frequencies Som+ mediated inhibition would be increased relative to Parv+. The synaptic mechanisms underlying these changes appeared to be primarily presynaptic release probability and synapse number, as opposed to postsynaptic strength. Overall, our data illustrate that activity dependent regulation of inhibition differs depending on cell type, which may be related to the different functions of these neurons.

A number of studies have examined activity-dependent, homeostatic regulation of synaptic and neuronal function. However, none have used paired recordings of synaptically coupled neurons involving identified inhibitory neuron types. Paired recordings allow a careful examination of evoked transmission of isolated, synaptically coupled neurons of known type. In addition, most studies have used dissociated neuron culture where, unlike the slice culture used here, circuit structure is not maintained.

Differential regulation of Parv+ and Som+ circuitry

Homeostatic regulation of recurrent inhibition provided by Parv+ and Som+ neurons had two key differences. First, uIPSCs originating from Parv+ neurons were decreased while those from Som+ neurons were unchanged (Fig. 2). Moreover, the duration of uIPSCs from Som+ neurons was increased by 22% suggesting that the net inhibitory charge provided by Som+ neurons may actually increase. Som+ inhibitory synapses preferentially target the dendrites of excitatory neurons (Di Cristo et al. 2004; Somogyi et al. 1998) indicating that aspects of dendritic inhibition may be paradoxically increased with activity blockade – an apparent nonhomeostatic adaptation. Because excitatory synaptic drive targeting excitatory neurons increases after chronic blockade (Turrigiano et al. 1998), increases in inhibition provided by Som+ neurons may increase in an effort to maintain a balance of inhibition and excitation in the dendrites.

Second, both uEPSCs and uIPSCs in Som+ circuitry underwent a shift in short-term plasticity while no such change occurred in Parv+ circuitry (in the context of short stimulus trains, Fig. 3,4). These adaptations indicate that a frequency-dependent shift occurs in the relative contribution of Parv+ and Som+ recurrent inhibition where Som+ inhibition is increased at lower frequency transmission. Recruitment of Som+ cell activity requires high frequency firing of excitatory neurons and the subsequent facilitation of excitatory synapses (Gibson et al. 1999; Reyes et al. 1998). Therefore, the frequency-dependent adaptation of Som+ synapses may be important to maintain any Som+ recurrent inhibition during low network activity as well as keep the proper balance of Parv+ and Som+ when activity is chronically decreased.

The synapses of Parv+ neurons are known to preferentially target the soma and proximal dendrites while synapses of Som+ neurons preferentially target distal dendrites (Di Cristo et al. 2004; Somogyi et al. 1998). Because of this differential targeting, the relative increase in Som+ inhibition at low frequencies would translate to a similar increase in distal or dendritic inhibition.

In hippocampus, it has been demonstrated that low frequency activity induces greater inhibition at the soma and high frequency activity induces greater inhibition in dendrites (Pouille and Scanziani 2004), and it is likely that this distinction is due to Parv+ and Som+ neurons, respectively. Therefore, our results suggest that the transition frequency from somatic to dendritic inhibition is reduced when activity levels are decreased, thereby changing information processing of disynaptic inhibitory circuitry.

Mechanistic alterations at both Parv+ and Som+ inhibitory synapses are similar, but result in different functional consequences

Our data indicate that activity blockade induces both an increase in release probability and a decrease in synapse number at both Parv+ and Som+ inhibitory synapse subtypes. These are opposing effects that almost completely offset each other at Som+ inhibitory connections and only partially offset each other at Parv+ connections (Fig. 7). Hence, different functional outcomes occur at this two synapse types although the same underlying synaptic changes appear to be occurring.

The decreases in synapse number were revealed at Parv+ inhibitory synapses by a decrease in connectivity with excitatory postsynaptic target (Fig. $2A_2$). This is consistent with an earlier anatomical study performing the identical experiment (same age, except in visual cortex slice cultures) where Parv+ bouton number was decreased approximately 50% after 5 day TTX treatment (Chattopadhyaya et al. 2004). This value closely matches the drop in Parv+ uIPSCs when we removed the offsetting effect of release probability (52%, Fig. 7D), supporting the assertion of a synapse number decrease. The decrease in Som+ inhibitory synapse number was observed directly by counting their boutons. Decreased immunocytochemical inhibitory synapse markers after TTX treatment have been reported in dissociated cultures (Hartman et al. 2006;

Kilman et al. 2002), but these studies did not distinguish between different inhibitory subtypes or make a link with evoked transmission.

Activity blockade also resulted in an apparent increase presynaptic release probability at inhibitory synapses that was observed by changes in short-term synaptic plasticity of Som+ uIPSCs in response to short trains of stimulation (Fig. 4B) and of Parv+ uIPSCs in response to long trains of stimulation (>150 APs; Fig. 7C). Our assertion that release probability is increased at inhibitory synapses with activity blockade is mainly based on short-term plasticity measurements, and therefore, we cannot completely rule out other pre- or postsynaptic mechanisms. The more pronounced decrease in Parv+ uIPSC amplitude measured in high Ca^{2+} after activity blockade is consistent with an increase in release probability (Fig. 7D).

Unchanged Parv+ IPSC quantal size (Fig. 7B) is in contrast with findings of increased inhibitory quantal size in dissociated cultures undergoing chronic TTX treatment (Hartman et al. 2006; Kilman et al. 2002). Several differences may account for this: 1) type (dissociated vs. slice culture) and age of culture (Burrone et al. 2002; Chattopadhyaya et al. 2004; De Simoni et al. 2003; Hartman et al. 2006; Wierenga et al. 2006), 2) treatment length (5 vs. 2 days), and 3) more specific identification of inhibitory subtype in this study. Because quantal events could not be resolved at Som+ inhibitory synapses, we cannot rule out a postsynaptic efficacy change at this connection.

Activity blockade causes similar increases in excitatory synaptic drive onto Parv+ and Som+ inhibitory neurons

As previously observed at excitatory neurons, excitatory synaptic drive onto both Parv+ and Som+ inhibitory neurons increased in response to activity blockade (Fig. 1) (Lissin et al. 1998; Murthy et al. 2001; Turrigiano et al. 1998). Interestingly, it was reported that inhibitory neurons do not show excitatory drive changes with activity blockade when only mEPSCs are

examined (Turrigiano et al. 1998)(also shown in Fig. $5A_2$,B_2). This highlights the importance of using paired recordings to examine evoked transmission since we were able to discern changes with this method.

We focused on mechanisms underlying the increase in excitatory drive onto Som+ neurons since this connection was most amenable to investigation. Similar to inhibitory synapses, activity blockade resulted in changes in presynaptic release probability and synapse number, as opposed to quantal content. At Som+ neurons uEPSC increases are likely to be due to increases in both presynaptic release probability and synapse number as revealed by altered short term plasticity (Figs. 3,6) and increased percent connectivity (Fig. $5B_1$), respectively. Decreases in failure rate and CV (Fig. 6) support an increase in release probability, synapse number, or both. In contrast, short-term plasticity of uEPSCs onto Parv+ neurons was unaffected by activity blockade suggesting no change in release probability occurred (Watanabe et al. 2005), but connectivity frequency did increase suggesting an increase in synapse number (Figs. $3A_2$,$5A_1$). The increased release probability at excitatory synapses targeting Som+ neurons is consistent with more direct measurements of increased release at excitatory synapses targeting hippocampal excitatory neurons after chronic TTX treatment (Murthy et al. 2001).

The effects of activity blockade are likely not due to cell or dendritic size changes

It is unlikely that uEPSC alterations are a secondary effect due to morphological changes in inhibitory neurons. There are no alterations in the Som+ dendritic tree with TTX-treatment of slightly shorter duration (4 days) (Gibson et al. 2006). Similarly, Parv+ neurons do not display any gross alterations in soma size or in dendritic and axonal arbors after 5 days of TTX treatment in visual cortical slice culture at our experimental age (Chattopadhyaya et al. 2004). We found no change in membrane capacitance of Parv+ or Som+ neurons suggesting that cell size was unchanged.

A possible morphological alteration in excitatory neurons is suggested by the 26% decrease in total membrane capacitance of excitatory neurons – an indication that these cells may be slightly smaller. But this change cannot fully explain why we observe differential regulation of amplitude or of short-term plasticity at Parv+ and Som+ inhibitory synapses.

Universal aspects of cortical homeostasis and the control of network activity

In response to activity blockade, excitatory neurons undergo an increase in their excitatory drive and in their intrinsic excitability (Desai et al. 1999b; Murthy et al. 2001; Turrigiano et al. 1998). Here, we demonstrate that inhibitory neurons display the same adaptations suggesting that these are universal adaptations for firing rate made among most cell types in cortex. Assuming that homeostatic regulation is intended to maintain firing at some set-point, all cells appear to adapt to chronic decreases in activity by facilitating their firing to regain this set-point.

If the same upregulation of activity occurs in both excitatory and inhibitory neurons, how is network activity increased after blockade? And how are the principal players in information processing and relay (the excitatory neurons) regulated in this scenario? Network activity increases in spite of inhibitory circuitry activity being promoted (Corner and Ramakers 1992; Gibson et al. 2006; Turrigiano et al. 1998). The critical point of regulation may be at the inhibitory synapse, and according to our study, the Parv+ inhibitory synapse. Because activity blockade induces a decrease in monosynaptic Parv+ inhibition (as described here) and an increase in monosynaptic excitation (Turrigiano et al. 1998), there is a net increase in the excitatory-to-inhibitory ratio impinging on excitatory neurons which could underlie the increase in network activity. Parv+ synapses are optimally positioned to gate and control action potential generation at excitatory neurons since they target the soma and proximal dendrites (Somogyi et al. 1998). Therefore, regulation of Parv+ inhibitory synapses provide an effective means to control the

firing output of the principal neurons (the excitatory neurons) (Miles et al. 1996) and is an effective site for homeostatic regulation of activity.

Figure Legends

Figure 1. Consistent with homeostatic regulation in inhibitory neurons, chronic activity blockade enhances excitatory drive onto both inhibitory neuron subtypes. A_1,B_1) Unitary EPSCs (uEPSCs) evoked from excitatory neurons (E) were examined in neighboring Parv+ (P) and Som+ (S) inhibitory neurons. Above: Example of a presynaptic action potential (AP, truncated vertically). Below: uEPSCs evoked in control and TTX-treated cultures. A_2,B_2) Percent connected of all test pairs is decreased for Parv+ but not for Som+ circuitry (but see Fig. 5A with larger data set). A_3,B_3) Average uEPSC1 (first uEPSC in a train) amplitude was dramatically increased in both subtypes. A_4,B_4) Net excitatory drive, the average of both connected and nonconnected (0 pA) pairs, was increased at both subtypes. Scale bars: Vertical, 700 and 10 pA for APs and PSCs, respectively. Horizontal, 50 ms. * $p<0.03$. Sample number indicated in bars.

Figure 2 Chronic activity blockade differentially regulates inhibitory synaptic drive onto excitatory neurons. A_1,B_1) uIPSCs were evoked from Parv+ (P) and Som+ (S) neurons and examined in neighboring excitatory neurons (E). Parv+ uIPSCs were recorded using "high Cl" pipette solution, and hence displayed downward waveforms. A_2,B_2) Percent connected of Parv+ uIPSCs, but not Som+ uIPSCs, is decreased with chronic blockade (Chi-Sqr). A_3,B_3) When a connection existed, average uIPSC1 amplitude was not affected for either inhibitory connection type. A_4,B_4) Net inhibitory drive was only decreased for Parv+ mediated uIPSCs. Scale bars: Vertical, 700 and 10 pA for APs and PSCs, respectively. Horizontal, 50 ms. * $p<0.05$.

Figure 3. Short-term plasticity is differentially regulated at excitatory synapses. A_1,B_1) Recordings of uEPSC trains. A_2,B_2) Som+ uEPSCs became more depressing with TTX treatment while no change was detected in Parv+ uEPSCs. Only amplitudes from last 3 uEPSCs shown.

A_3,B_3) Net excitatory drive at uEPSC5 was increased for both inhibitory neuron subtypes. Scale bars: Vertical, 500 and 10 pA. Horizontal, 50 ms. * $p<0.02$, ** $p<0.004$.

Figure 4. Chronic activity blockade differentially regulates short-term plasticity of uIPSCs. A_1,B_1) uIPSC trains were evoked by trains of presynaptic action potentials (top). A_2,B_2) While short-term plasticity is unaltered with Parv+ uIPSCs, Som+ uIPSCs become dramatically more depressing. A_3,B_3) Net drive for uIPSC8 is decreased at Parv+, but not Som+, synapses. Scale bars: Vertical, 5 pA. Horizontal, 50 ms. * $p<0.004$.

Figure 5. Increased connectivity suggests an increase in synapse number mediating the increase in uEPSC drive. A_1,B_1) An increase in percent connected for all tested pairs suggests that increased synapse number is involved in the uEPSC increase. A_2,B_2) No changes were observed in mEPSC properties.

Figure 6. Increased quantal content, not quantal size, mediating the increased strength of uEPSCs targeting Som+ neurons. A) CV and B) failures of uEPSCs are decreased with activity blockade suggesting increased quantal content. C) An experiment from control slices where Sr^{2+} was substituted for Ca^{2+} to induce asynchronous release. The AP shown is the last in a train of 15. The EPSC in the control trace is truncated. D) A small decrease in quantal size after chronic TTX treatment indicates that changes in synaptic efficacy, and probably postsynaptic receptor function, do not account for the increased excitatory drive. Scale bars: Vertical, 1000 and 10 pA. Horizontal, 50 ms. * $p<0.05$.

Figure 7. With Parv+ uIPSCs, activity blockade does not affect quantal size but increases release probability. A) Percent connected is decreased in all experiments performed examining Parv+ uIPSCs suggesting fewer synaptic contacts. B) Sr^{2+} was substituted for Ca^{2+} to

induce asynchronous release and enable the measurement of quantal events directly mediating uIPSCs. The trace epoch shown occurs during the last 3 action potentials in a train of 15. Quantal size was unchanged with TTX treatment suggesting that regulation does not involve a postsynaptic efficacy mechanism (n=22,20). Slashes represent 350 ms of omitted trace. Scale bars: Vertical, 500 and 5 pA. Horizontal, 50 ms. C) Long stimulus trains are more depressing after 5 day TTX treatment suggesting an increase in release probability (n=14,12). * $p<0.05$, calculated with repeated measures ANOVA D) When release probability is increased to diminish the role of increased release probability, a decrease in uIPSC amplitude emerges (K-Gluc pipette solution used so currents are outward). Scale bars: Vertical, 10 pA. Horizontal, 50 ms. * $p<0.03$.

Figure 8. A decrease in Som+ inhibitory "putative" boutons and synaptic contacts. A) No change in the percent connected for Som+-mediated uIPSCs after chronic activity for all pairs recorded. B) Images of presynaptic axons and boutons (GFP) and postsynaptic excitatory neuron dendrites (DsRed). Putative contacts are indicated by arrow heads. Some axons travel in and out of the image plane. Image is a superposition of images creating a 4.8 um thick section, and hence some colocalized spots are not putative contacts because they are separated by more than 0.5 μm in depth. Scale bars, 5μm. C) The GFP intensity distribution along an axon shows periodic increases that we define as "putative" presynaptic boutons. Dotted and solid horizontal lines represent baseline and threshold intensity levels. D) The density of "putative" presynaptic boutons is decreased with activity blockade (n=29,20 images). E) Intensity distributions of DsRed (red) and GFP (green) at a "putative" synaptic contact. Vertical dashed lines show the amount of overlap among the two distributions. F)"Putative" synaptic contacts are decreased, also (n=16,13 cells) * $p<0.02$.

Abbott LF, Varela JA, Sen K, and Nelson SB. Synaptic depression and cortical gain control. *Science* 275: 220-224, 1997.

Beierlein M, Gibson JR, and Connors BW. Two dynamically distinct inhibitory networks in layer 4 of the neocortex. *J Neurophysiol* 90: 2987-3000, 2003.
Burrone J, O'Byrne M, and Murthy VN. Multiple forms of synaptic plasticity triggered by selective suppression of activity in individual neurons. *Nature* 420: 414-418., 2002.
Calakos N, Schoch S, Sudhof TC, and Malenka RC. Multiple roles for the active zone protein RIM1alpha in late stages of neurotransmitter release. *Neuron* 42: 889-896, 2004.
Chattopadhyaya B, Di Cristo G, Higashiyama H, Knott GW, Kuhlman SJ, Welker E, and Huang ZJ. Experience and activity-dependent maturation of perisomatic GABAergic innervation in primary visual cortex during a postnatal critical period. *J Neurosci* 24: 9598-9611, 2004.
Corner MA and Ramakers GJ. Spontaneous firing as an epigenetic factor in brain development--physiological consequences of chronic tetrodotoxin and picrotoxin exposure on cultured rat neocortex neurons. *Brain Res Dev Brain Res* 65: 57-64., 1992.
Davis GW and Goodman CS. Genetic analysis of synaptic development and plasticity: homeostatic regulation of synaptic efficacy. *Curr Opin Neurobiol* 8: 149-156, 1998.
De Simoni A, Griesinger CB, and Edwards FA. Development of rat CA1 neurones in acute versus organotypic slices: role of experience in synaptic morphology and activity. *J Physiol* 550: 135-147, 2003.
Desai NS, Cudmore RH, Nelson SB, and Turrigiano GG. Critical periods for experience-dependent synaptic scaling in visual cortex. *Nat Neurosci* 5: 783-789., 2002.
Desai NS, Rutherford LC, and Turrigiano GG. BDNF regulates the intrinsic excitability of cortical neurons. *Learn Mem* 6: 284-291., 1999a.
Desai NS, Rutherford LC, and Turrigiano GG. Plasticity in the intrinsic excitability of cortical pyramidal neurons. *Nat Neurosci* 2: 515-520., 1999b.
Di Cristo G, Wu C, Chattopadhyaya B, Ango F, Knott G, Welker E, Svoboda K, and Huang ZJ. Subcellular domain-restricted GABAergic innervation in primary visual cortex in the absence of sensory and thalamic inputs. *Nat Neurosci* 7: 1184-1186, 2004.
Dumitriu D, Cossart R, Huang J, and Yuste R. Correlation between axonal morphologies and synaptic input kinetics of interneurons from mouse visual cortex. *Cereb Cortex* 17: 81-91, 2007.
Echevarria D and Albus K. Activity-dependent development of spontaneous bioelectric activity in organotypic cultures of rat occipital cortex. *Brain Res Dev Brain Res* 123: 151-164, 2000.
Faber DS and Korn H. Applicability of the coefficient of variation method for analyzing synaptic plasticity. *Biophys J* 60: 1288-1294, 1991.
Feldmeyer D, Egger V, Lubke J, and Sakmann B. Reliable synaptic connections between pairs of excitatory layer 4 neurones within a single 'barrel' of developing rat somatosensory cortex. *J Physiol* 521 Pt 1: 169-190, 1999.
Feldmeyer D, Lubke J, Silver RA, and Sakmann B. Synaptic connections between layer 4 spiny neurone-layer 2/3 pyramidal cell pairs in juvenile rat barrel cortex: physiology and anatomy of interlaminar signalling within a cortical column. *J Physiol* 538: 803-822, 2002.
Gahwiler BH, Capogna M, Debanne D, McKinney RA, and Thompson SM. Organotypic slice cultures: a technique has come of age. *Trends Neurosci* 20: 471-477, 1997.

Gibson JR, Bartley AF, and Huber KM. Role for the subthreshold currents ILeak and IH in the homeostatic control of excitability in neocortical somatostatin-positive inhibitory neurons. *J Neurophysiol* 96: 420-432, 2006.
Gibson JR, Beierlein M, and Connors BW. Two networks of electrically coupled inhibitory neurons in neocortex. *Nature* 402: 75-79, 1999.
Gil Z, Connors BW, and Amitai Y. Efficacy of thalamocortical and intracortical synaptic connections: quanta, innervation, and reliability. *Neuron* 23: 385-397, 1999.
Gonchar Y and Burkhalter A. Three distinct families of GABAergic neurons in rat visual cortex. *Cereb Cortex* 7: 347-358, 1997.
Gorba T, Klostermann O, and Wahle P. Development of neuronal activity and activity-dependent expression of brain-derived neurotrophic factor mRNA in organotypic cultures of rat visual cortex. *Cereb Cortex* 9: 864-877., 1999.
Gupta A, Wang Y, and Markram H. Organizing principles for a diversity of GABAergic interneurons and synapses in the neocortex. *Science* 287: 273-278, 2000.
Haas K, Sin WC, Javaherian A, Li Z, and Cline HT. Single-cell electroporation for gene transfer in vivo. *Neuron* 29: 583-591, 2001.
Hartman KN, Pal SK, Burrone J, and Murthy VN. Activity-dependent regulation of inhibitory synaptic transmission in hippocampal neurons. *Nat Neurosci* 9: 642-649, 2006.
Hendry SH and Jones EG. Activity-dependent regulation of GABA expression in the visual cortex of adult monkeys. *Neuron* 1: 701-712, 1988.
Horton JC and Hubel DH. Regular patchy distribution of cytochrome oxidase staining in primary visual cortex of macaque monkey. *Nature* 292: 762-764, 1981.
Kilman V, van Rossum MC, and Turrigiano GG. Activity deprivation reduces miniature IPSC amplitude by decreasing the number of postsynaptic GABA(A) receptors clustered at neocortical synapses. *J Neurosci* 22: 1328-1337., 2002.
Kraushaar U and Jonas P. Efficacy and stability of quantal GABA release at a hippocampal interneuron-principal neuron synapse. *J Neurosci* 20: 5594-5607., 2000.
Kumar SS, Bacci A, Kharazia V, and Huguenard JR. A developmental switch of AMPA receptor subunits in neocortical pyramidal neurons. *J Neurosci* 22: 3005-3015., 2002.
Lissin DV, Gomperts SN, Carroll RC, Christine CW, Kalman D, Kitamura M, Hardy S, Nicoll RA, Malenka RC, and von Zastrow M. Activity differentially regulates the surface expression of synaptic AMPA and NMDA glutamate receptors. *Proc Natl Acad Sci U S A* 95: 7097-7102., 1998.
Luthi A, Di Paolo G, Cremona O, Daniell L, De Camilli P, and McCormick DA. Synaptojanin 1 contributes to maintaining the stability of GABAergic transmission in primary cultures of cortical neurons. *J Neurosci* 21: 9101-9111., 2001.
Maffei A, Nataraj K, Nelson SB, and Turrigiano GG. Potentiation of cortical inhibition by visual deprivation. *Nature* 443: 81-84, 2006.
Maffei A, Nelson SB, and Turrigiano GG. Selective reconfiguration of layer 4 visual cortical circuitry by visual deprivation. *Nat Neurosci* 7: 1353-1359, 2004.
Marder E and Prinz AA. Modeling stability in neuron and network function: the role of activity in homeostasis. *Bioessays* 24: 1145-1154, 2002.
Markram H, Lubke J, Frotscher M, Roth A, and Sakmann B. Physiology and anatomy of synaptic connections between thick tufted pyramidal neurones in the developing rat neocortex. *J Physiol* 500 (Pt 2): 409-440, 1997.

Marty S, Berzaghi Mda P, and Berninger B. Neurotrophins and activity-dependent plasticity of cortical interneurons. *Trends Neurosci* 20: 198-202., 1997.
Marty S, Wehrle R, and Sotelo C. Neuronal activity and brain-derived neurotrophic factor regulate the density of inhibitory synapses in organotypic slice cultures of postnatal hippocampus. *J Neurosci* 20: 8087-8095., 2000.
Micheva KD and Beaulieu C. Neonatal sensory deprivation induces selective changes in the quantitative distribution of GABA-immunoreactive neurons in the rat barrel field cortex. *J Comp Neurol* 361: 574-584, 1995.
Miles R, Toth K, Gulyas AI, Hajos N, and Freund TF. Differences between somatic and dendritic inhibition in the hippocampus. *Neuron* 16: 815-823., 1996.
Murthy VN, Schikorski T, Stevens CF, and Zhu Y. Inactivity produces increases in neurotransmitter release and synapse size. *Neuron* 32: 673-682., 2001.
Musleh W, Bi X, Tocco G, Yaghoubi S, and Baudry M. Glycine-induced long-term potentiation is associated with structural and functional modifications of alpha-amino-3-hydroxyl-5-methyl-4-isoxazolepropionic acid receptors. *Proc Natl Acad Sci U S A* 94: 9451-9456, 1997.
Oliva AA, Jr., Jiang M, Lam T, Smith KL, and Swann JW. Novel hippocampal interneuronal subtypes identified using transgenic mice that express green fluorescent protein in GABAergic interneurons. *J Neurosci* 20: 3354-3368., 2000.
Oliva AA, Jr., Lam TT, and Swann JW. Distally directed dendrotoxicity induced by kainic Acid in hippocampal interneurons of green fluorescent protein-expressing transgenic mice. *J Neurosci* 22: 8052-8062., 2002.
Patz S, Wirth MJ, Gorba T, Klostermann O, and Wahle P. Neuronal activity and neurotrophic factors regulate GAD-65/67 mRNA and protein expression in organotypic cultures of rat visual cortex. *Eur J Neurosci* 18: 1-12., 2003.
Pouille F and Scanziani M. Routing of spike series by dynamic circuits in the hippocampus. *Nature* 429: 717-723, 2004.
Rae JL and Levis RA. Single-cell electroporation. *Pflugers Arch* 443: 664-670, 2002.
Rathenberg J, Nevian T, and Witzemann V. High-efficiency transfection of individual neurons using modified electrophysiology techniques. *J Neurosci Methods* 126: 91-98, 2003.
Reim K, Mansour M, Varoqueaux F, McMahon HT, Sudhof TC, Brose N, and Rosenmund C. Complexins regulate a late step in Ca2+-dependent neurotransmitter release. *Cell* 104: 71-81, 2001.
Reyes A, Lujan R, Rozov A, Burnashev N, Somogyi P, and Sakmann B. Target-cell-specific facilitation and depression in neocortical circuits. *Nature Neurosci* 1: 279-285, 1998.
Sara Y, Virmani T, Deak F, Liu X, and Kavalali ET. An isolated pool of vesicles recycles at rest and drives spontaneous neurotransmission. *Neuron* 45: 563-573., 2005.
Somogyi P, Tamas G, Lujan R, and Buhl EH. Salient features of synaptic organisation in the cerebral cortex. *Brain Res Brain Res Rev* 26: 113-135, 1998.
Stoppini L, Buchs PA, and Muller D. A simple method for organotypic cultures of nervous tissue. *J Neurosci Methods* 37: 173-182., 1991.
Stuart GJ, Dodt HU, and Sakmann B. Patch-clamp recordings from the soma and dendrites of neurons in brain slices using infrared video microscopy. *Pflugers Arch* 423: 511-518, 1993.

Tsodyks MV and Markram H. The neural code between neocortical pyramidal neurons depends on neurotransmitter release probability. *Proc Natl Acad Sci U S A* 94: 719-723, 1997.
Turrigiano GG. Homeostatic plasticity in neuronal networks: the more things change, the more they stay the same. *Trends Neurosci* 22: 221-227., 1999.
Turrigiano GG, Leslie KR, Desai NS, Rutherford LC, and Nelson SB. Activity-dependent scaling of quantal amplitude in neocortical neurons. *Nature* 391: 892-896, 1998.
Turrigiano GG and Nelson SB. Hebb and homeostasis in neuronal plasticity. *Curr Opin Neurobiol* 10: 358-364, 2000.
Turrigiano GG and Nelson SB. Homeostatic plasticity in the developing nervous system. *Nat Rev Neurosci* 5: 97-107, 2004.
Watanabe J, Rozov A, and Wollmuth LP. Target-specific regulation of synaptic amplitudes in the neocortex. *J Neurosci* 25: 1024-1033, 2005.
Welker E, Soriano E, and Van der Loos H. Plasticity in the barrel cortex of the adult mouse: effects of peripheral deprivation on GAD-immunoreactivity. *Exp Brain Res* 74: 441-452, 1989.
Wierenga CJ, Walsh MF, and Turrigiano GG. Temporal regulation of the expression locus of homeostatic plasticity. *J Neurophysiol* 96: 2127-2133, 2006.

Fig 1, Bartley

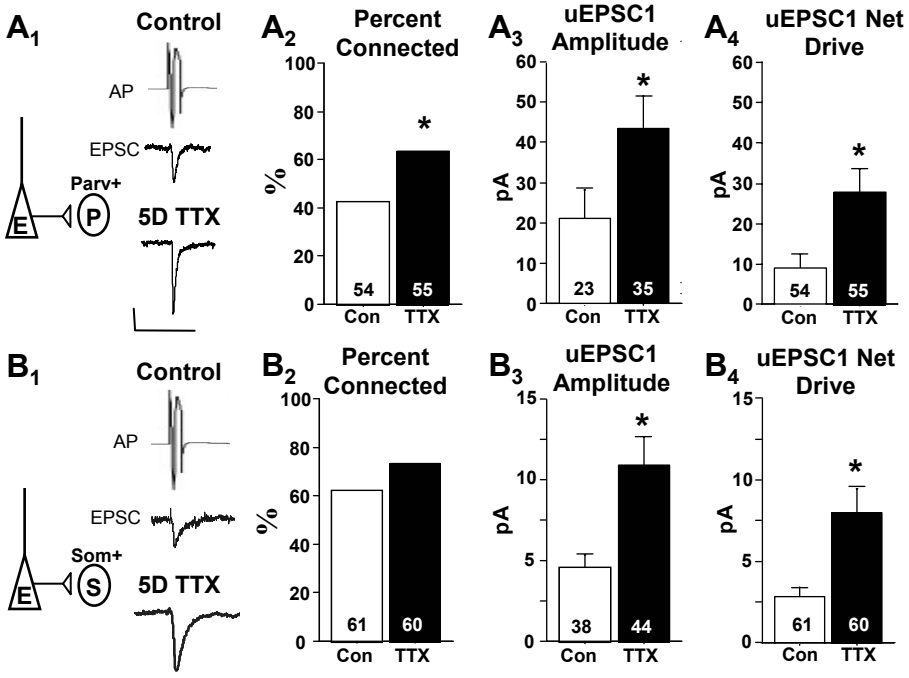

Fig 2, Bartley

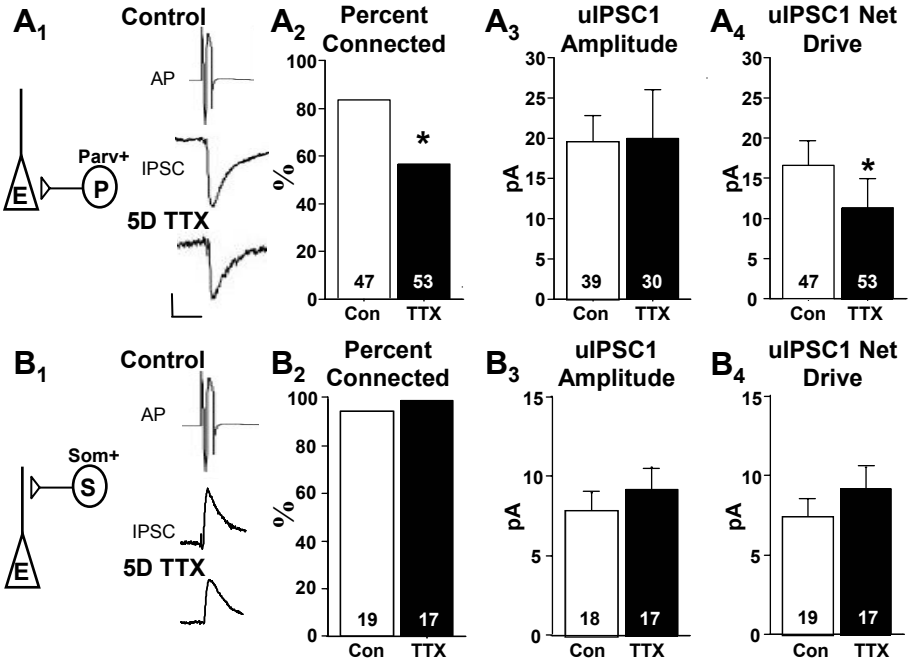

Fig 3, Bartley

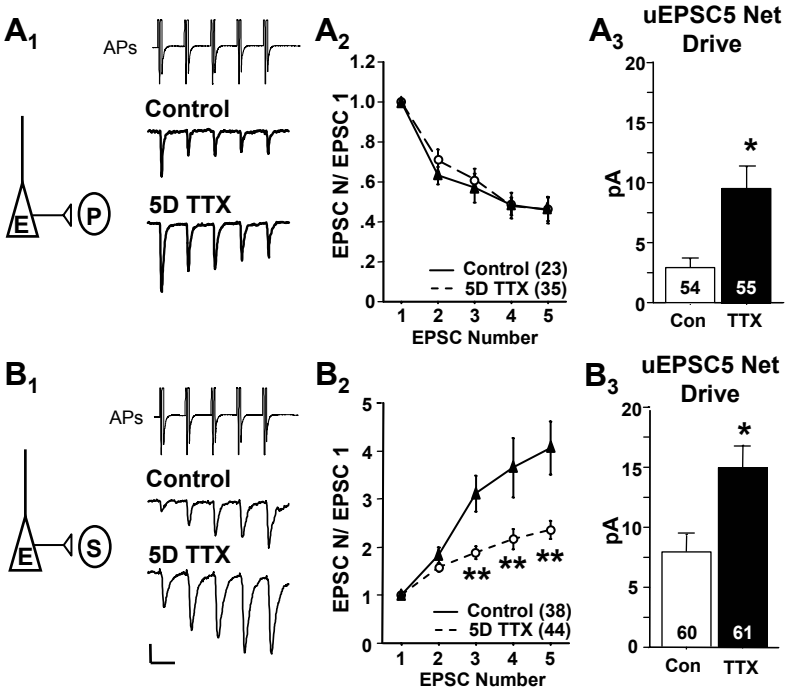

Fig 4, Bartley

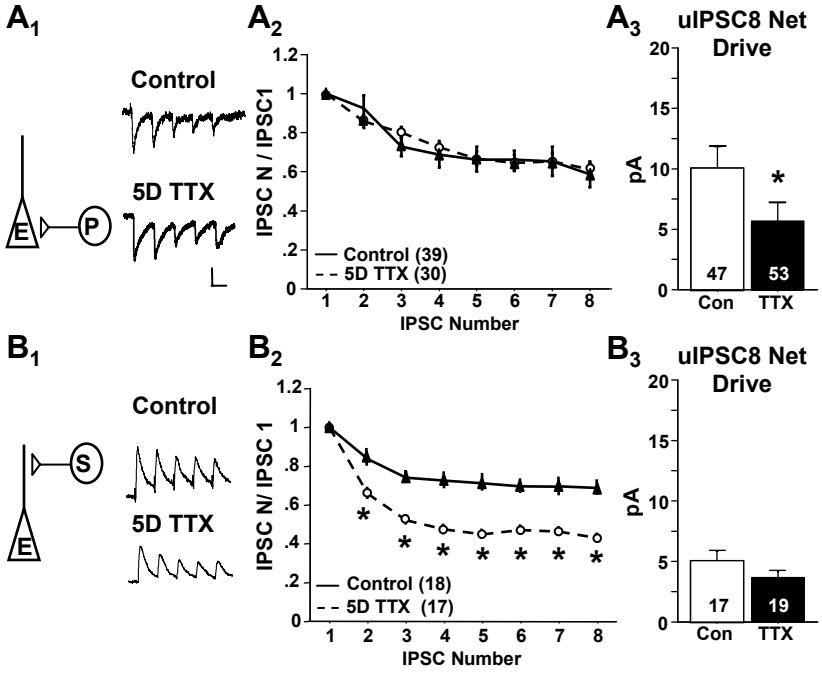

Fig 5, Bartley

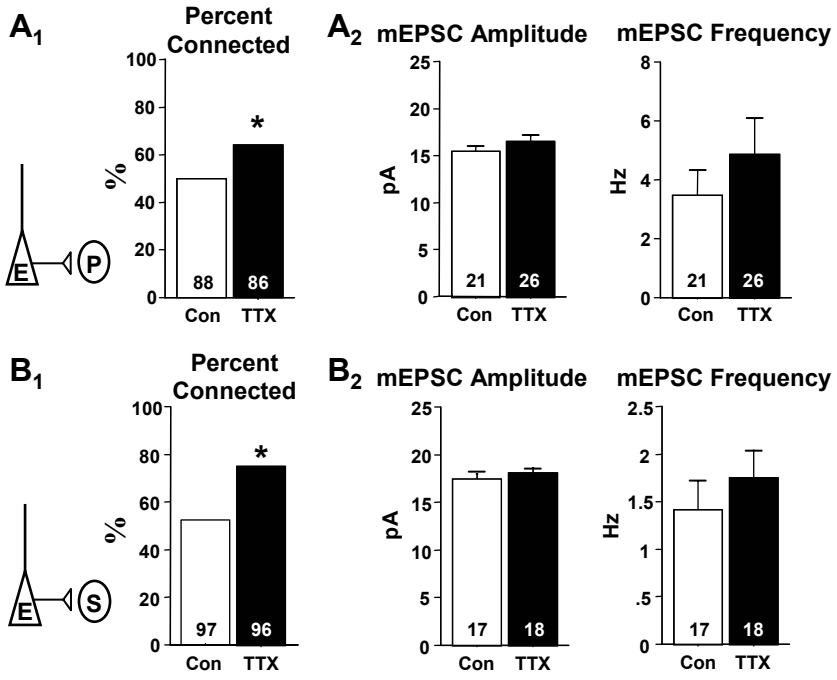

Fig 6, Bartley

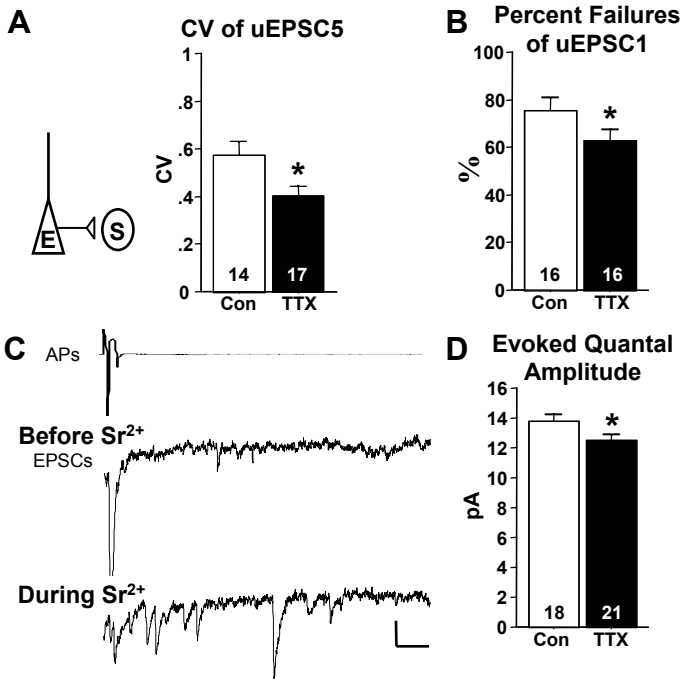

Fig 7, Bartley

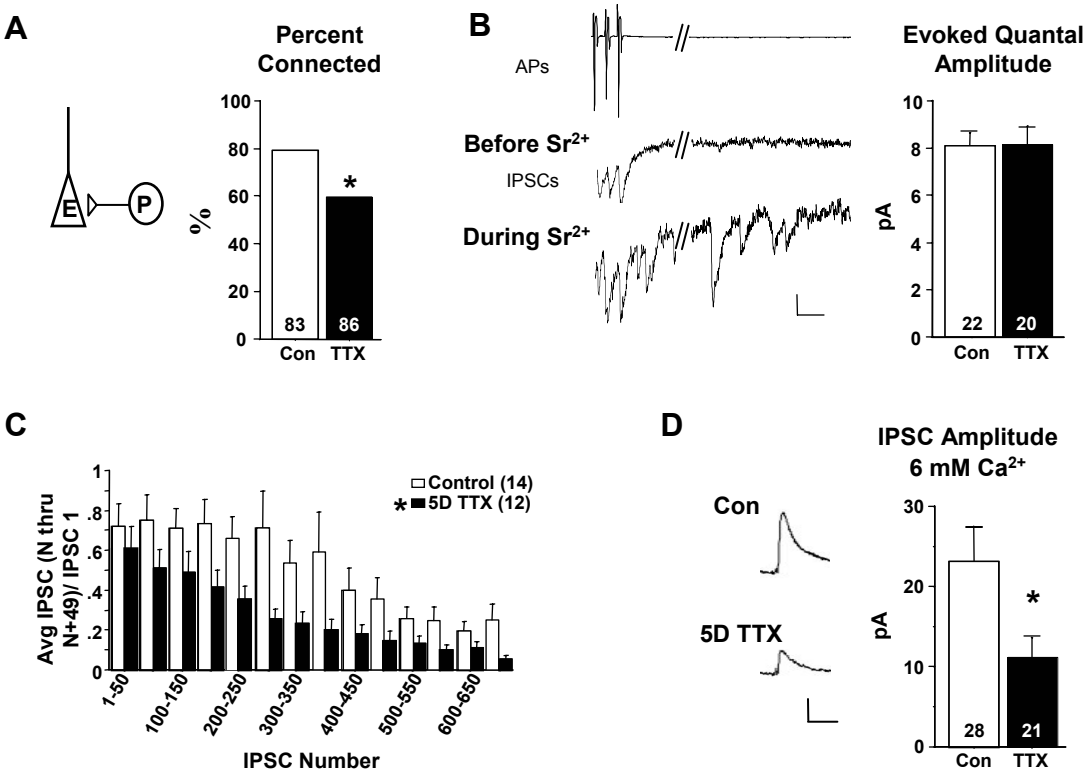

Fig 8, Bartley